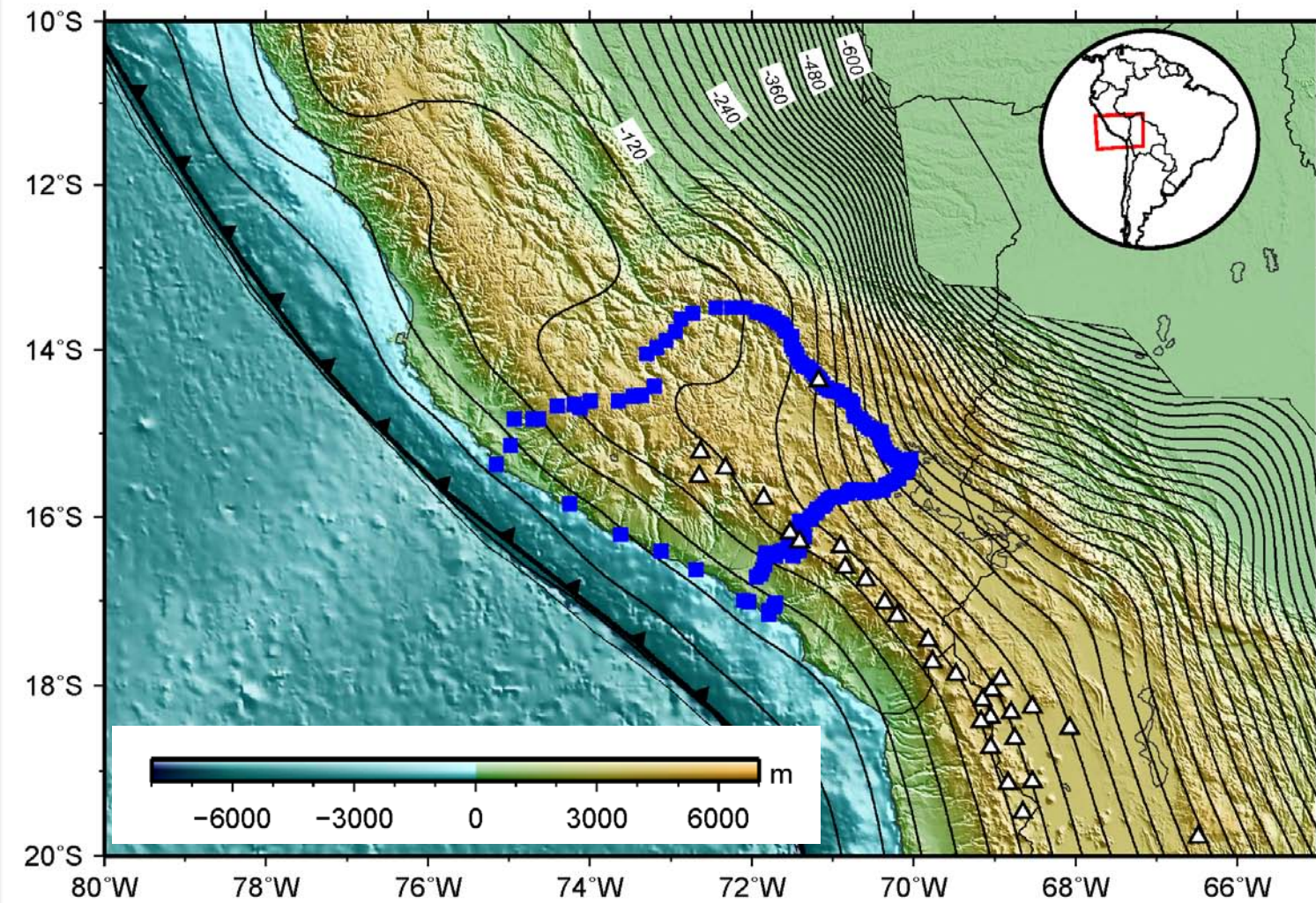


Surface Wave Tomography in Southern Peru

Yiran Ma (yrma@caltech.edu), Robert W. Clayton

Seismological Laboratory, California Institute of Technology, Pasadena, CA 91125

Introduction



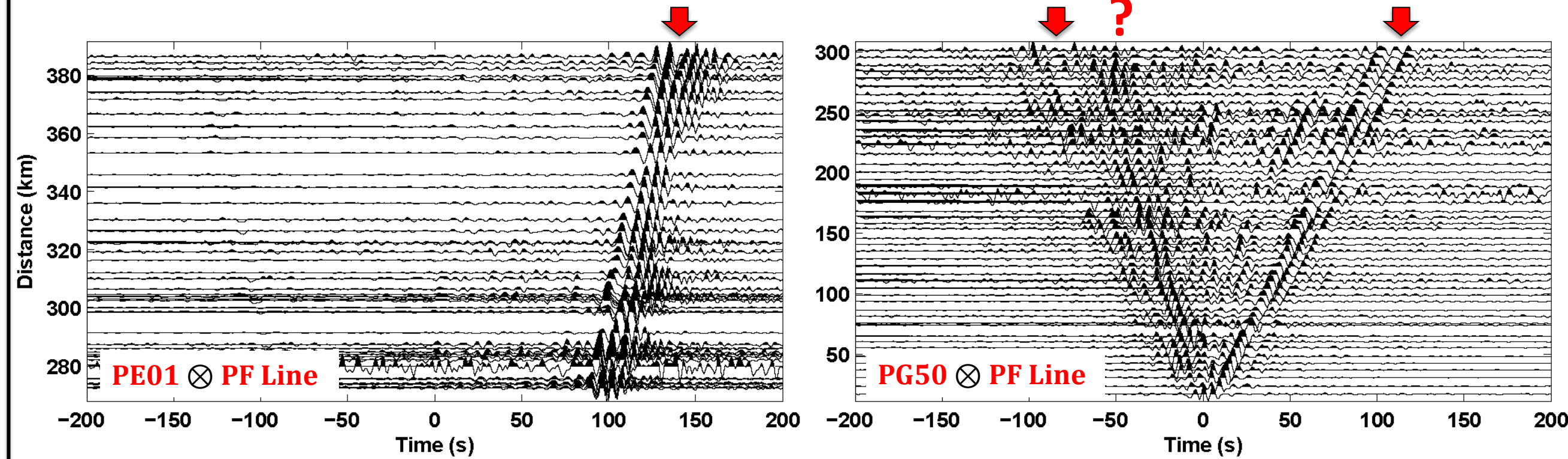
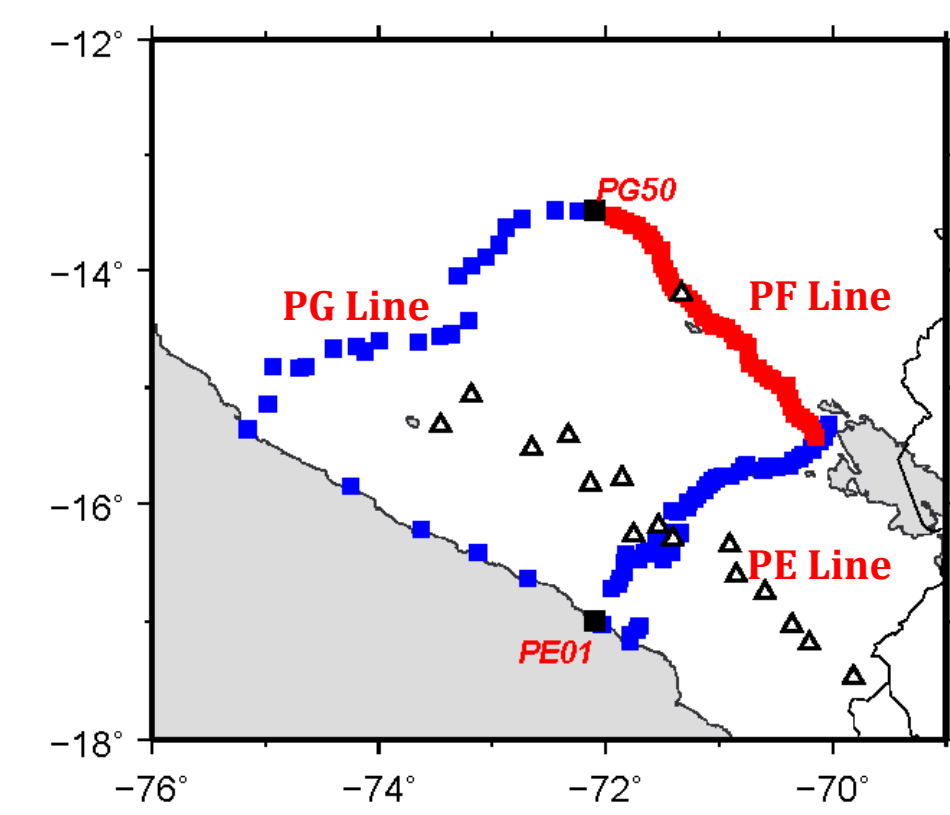
Southern Peru is an interesting area to study the subduction, orogeny and the related volcanism process along an active continental margin. The dip of the subducted Nazca slab changes from about 30° in the southeast to near horizontal in the northwest. Closely linked with the subduction process, the Altiplano-Puna plateau, the biggest continental plateau after Tibet correlates with the 30° dipping segment of the plate, and narrows considerably to the north. The Post-Pliocene volcanism also follows this correlation as is absent where the plate is nearly flat and well developed in the plateau where the plate is steeper.

To further the understanding of the structure in this region, a box-like array is deployed in progress above the transition zone from shallow subduction to dipping subduction. In this study, we use surface wave from the cross-correlations of ambient seismic noise (ASN) and teleseismic earthquakes to image the crust and upper mantle structure.

Ambient Noise Tomography

Noise Cross-correlation

We calculate the noise cross-correlations between velocity records and the results are the time derivative of the empirical Green's function. The cross-correlations in the direction perpendicular to the coast are one side for the dominant source from Pacific. In the direction parallel to the coast, two sides are observed. Interestingly, however, a signal ahead of the surface wave is also observed.



(Left) Noise cross-correlations in the direction perpendicular to the coast between PE01 and all the PF stations. (Right) Noise cross-correlation in the direction parallel to the coast between PG50 and all the PF stations. (Top right) Location of the stations.

Phase velocity Dispersion

We obtain high quality dispersion curves for period from 5 s to 30 s using the method by Yao *et al.* [2006], which is based on a far-field representation of the surface-wave Green's function and an image transformation technique. In the far field, the time harmonic wave of the Green's function for the surface wave fundamental mode at frequency ω is given by:

$$\text{Re}\{G_{AB}(\omega)\exp(-i\omega t)\} \approx C \cos(k_{AB}\Delta - \omega t + \frac{\pi}{4})$$

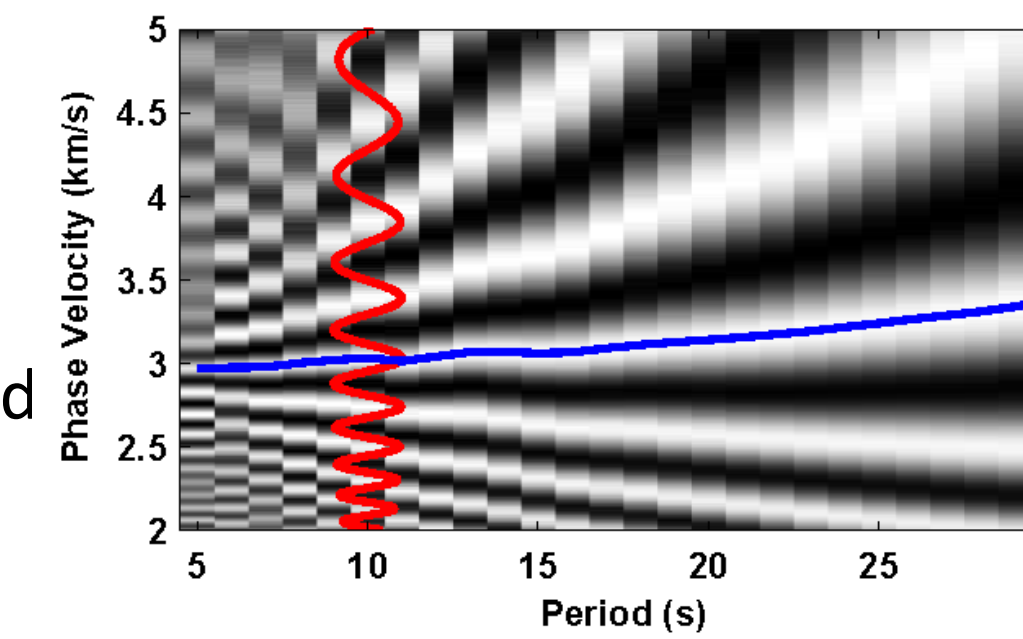
where C is a parameter related to the geometric spreading. When the travel time satisfies:

$$k_{AB}\Delta - \omega t + \frac{\pi}{4} = 0$$

It will correspond to one peak in the harmonic wave of the Green's function. The corresponding phase velocity is:

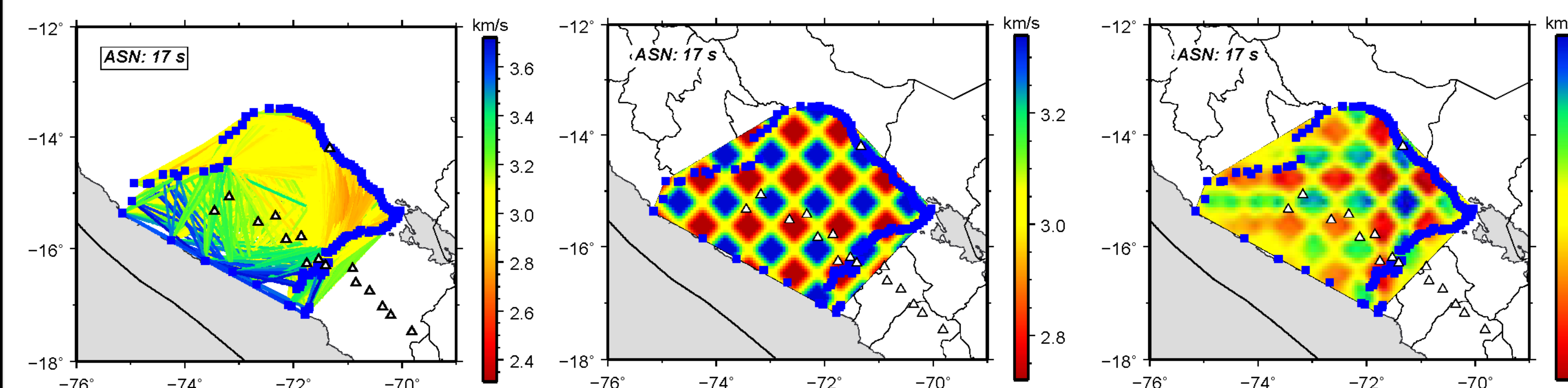
$$C_{AB} = \frac{\Delta}{t - \frac{\pi}{8}}$$

By transforming the t-T (travel time-period) diagram to c-T (phase velocity-period) diagram, we can pick a reasonable dispersion curve based on the priori information of the structure.

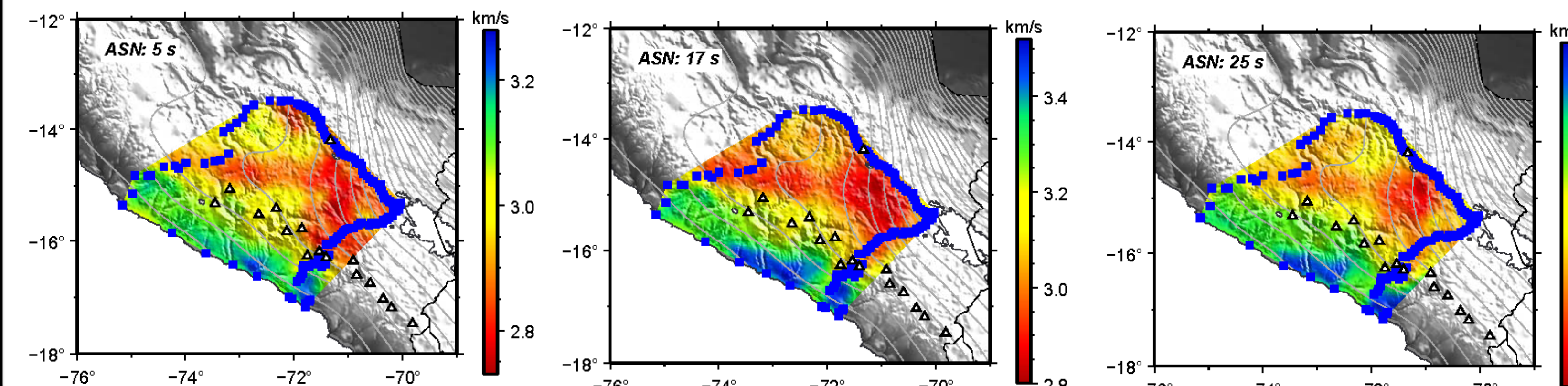


Phase velocity Tomography

We inverted the phase velocity dispersion curves to obtain velocity maps for each period. Here, we use a Cartesian geometry and equally-spaced nodes to parameterize the study region. Ray theory is used to trace the travel time between source and receiver. A least square solution is derived to minimize the penalty function including data misfit, smoothing constraint and ray coverage constraint.



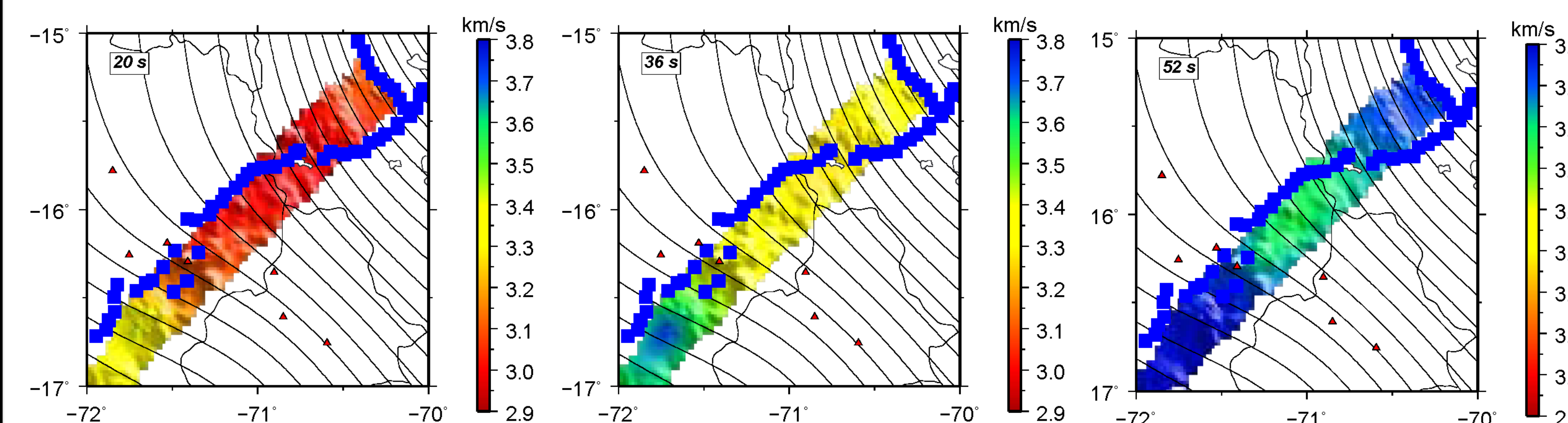
Take 17 s as an example. (Left) Ray coverage shaded with measured phase velocity. (Middle) Input model for checkerboard test. (Right) Output result calculated in the same scheme (grid size and damping parameters) as the real data.



Phase velocity map at 5 s, 17 s and 25 s. The forearc is higher in velocity than the back arc. The north of the backarc is higher in velocity than the southeast. A low velocity zone is located above the transition from flat to dipping subduction.

Earthquake Tomography

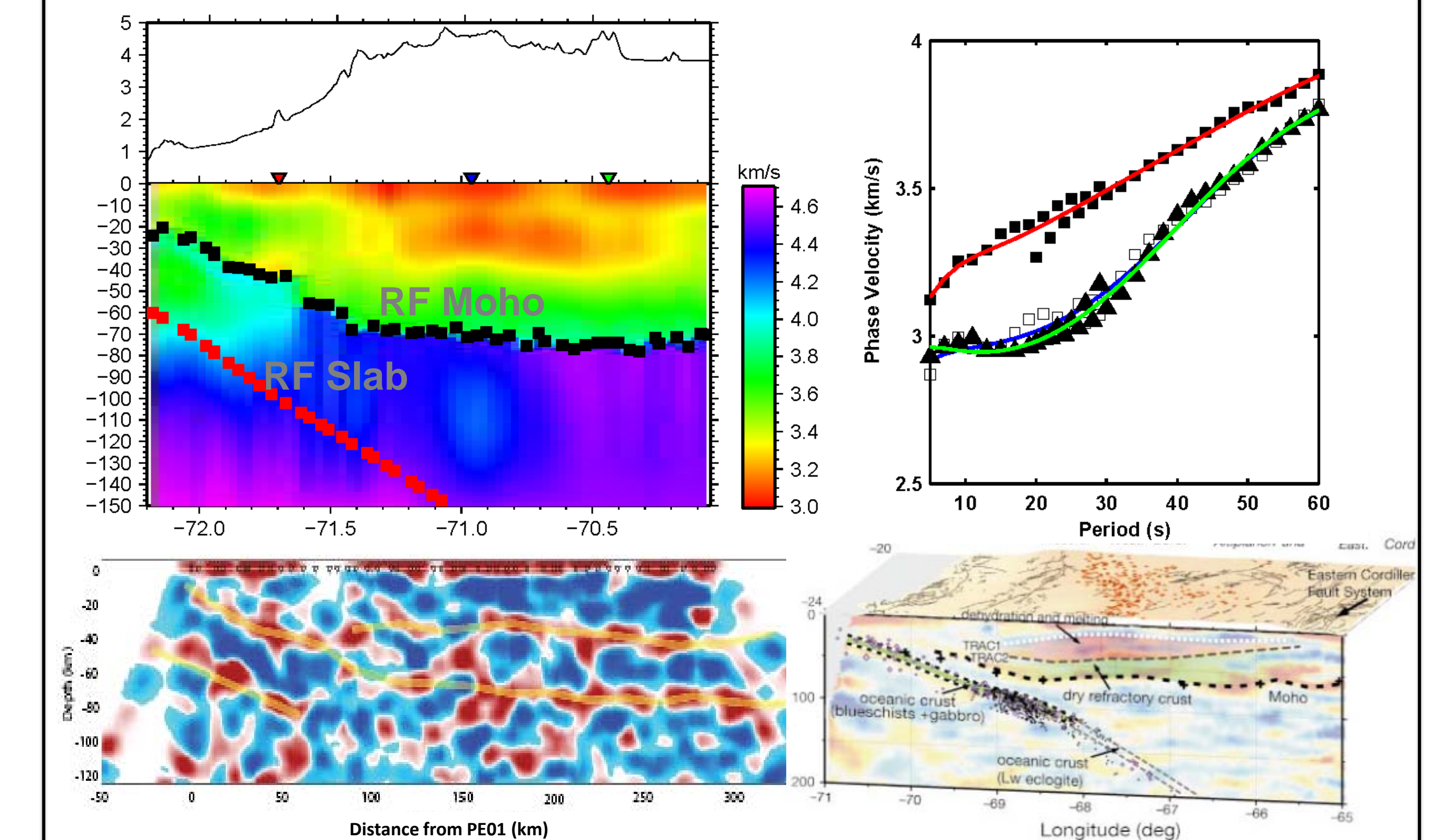
Because of the decreasing spectral power at long period (>20 s) and the two-wavelength interstation distance restriction for the ASN method, we use Two-station method [Yao *et al.*, 2006] to measure the phase velocity dispersion curves from 20 s to 60 s. We choose the two stations which are approximately on a great circle with earthquakes. The phase travel time for each period between the two stations is determined by the time shift at which the two narrow band-pass filtered waveforms reach the maximum correlation.



Phase velocity map at 20 s, 36 s and 52 s restricted to PE line (perpendicular to the coast above the dipping subduction) for the short of data coverage in the whole region.

Structure Inversion

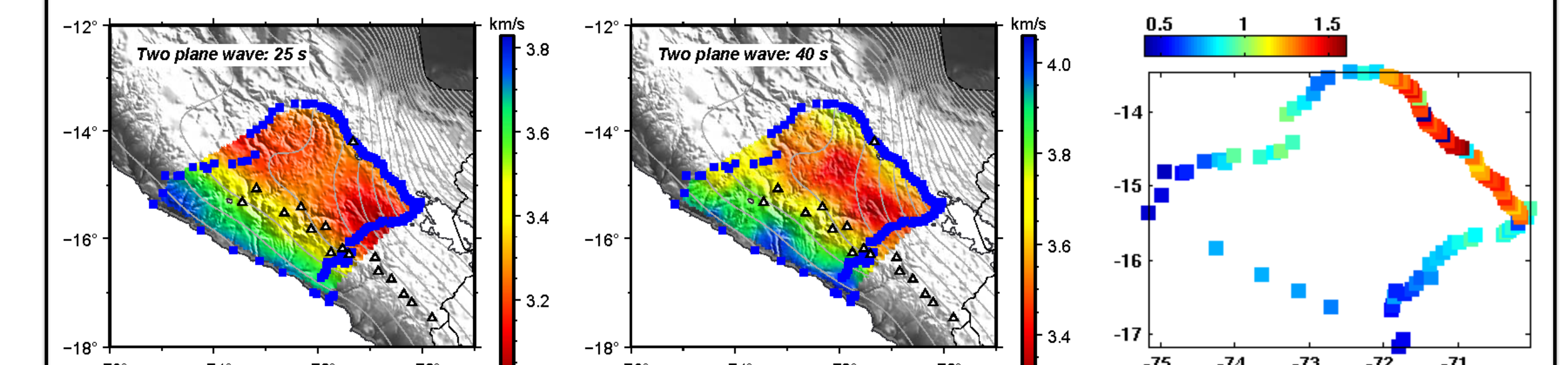
We do structure inversion along PE line which is perpendicular to the coast above the dipping subduction. We extract dispersion curves at the locations of each station from both ASN and earthquake tomography. The initial model has a linearly increasing velocity in the crust. The velocity gradient is calculated from Crust2.0 model, and the mantle velocity of the model is used here. The Moho depth is fixed by the receiver function results. The model is then discretized into 2 km thick layers. Finally, we invert for the S wave velocity in each layer from 0 to 150 km depth using the code by Herrmann and Ammon [2002].



(Top left) S wave velocity structure along the seismic line perpendicular to the coast above the dipping subduction. A low velocity layer is observed in the middle crust. (Top right) Example of the data extracted from the tomography maps at three locations annotated in the left figure. The solid lines are the fitted dispersion curve s from the inverted model. (Bottom left) Receiver function result [Philips, personal communication] along the same seismic line. A middle crust feature is also observed, which may be the converted phase from the bottom of the low velocity layer. (Bottom right) Receiver function result [Yuan *et al.*, 2000] about 6° south of the line, which also suggested a low velocity layer in the crust.

Two Plane Wave Inversion

To take into account the interference effects along the great circle path, and to make full use of the records at all stations, the Two-plane wave method [Yang and Forsyth, 2006] is used in addition to the Two-station method. The incoming wavefield is represented by two plane waves with unknown back azimuth, initial phase and amplitude. The six wave parameters, phase velocity structure, and the site effects on the amplitude of the records are inverted from the amplitude and phase at each period of the waveforms recorded by all stations.



(Left, middle) Phase velocity map inverted at 25 s and 40 s. (Right) Site response inverted to account for the mismatch using 2-D sensitivity kernels predicting the amplitude of the surface wave. Note the anti-correlation of the site response with the velocity.

References

- Yao, H., R. D. Van Der Hilst, and M. V. De Hoop (2006), Surface-wave array tomography in SE Tibet from ambient seismic noise and two-station analysis – I. Phase velocity maps, *Geophysical Journal International*, 166(2), 732-744.
Yuan, X., S. Sobolev, R. Kind, O. Oncken, G. Bock, G. Asch, B. Schurr, F. Graeber, A. Rudloff, and W. Hanka (2000), Subduction and collision processes in the Central Andes constrained by converted seismic phases, *Nature*, 408(6815), 958-961.
Yang, Y., and D. W. Forsyth (2006), Regional tomographic inversion of the amplitude and phase of Rayleigh waves with 2-D sensitivity kernels, *Geophysical Journal International*, 166(3), 1148-1160.